Integrated process for catalytic upgrading of hydrothermal liquefaction aqueous phase in the supercritical state

David H. Kenney[1], Alex Mosley[1], Oamfah Suwannapong[1],
Jia Yazon[1], C. P. Kelkar[2], Andrew J. Schmidt[3],
Geoffrey A. Tompsett[1], Alex R. Maag[1], Andrew R. Teixeira[1] and
Michael T. Timko[1]*

[1]Department of Chemical Engineering, Worcester Polytechnic Institute, Worcester, MA, United States,
[2]BASF Corporation, Iselin, NJ, United States, [3]Pacific Northwest National Laboratory, Chemical and
Biological Processes Development, Richland, WA, United States

Hydrothermal liquefaction (HTL) is a waste agnostic process that leverages near-critical water to break down macromolecules, forming an energy-dense biocrude. Some carbon contained in the waste feed is lost in the aqueous phase, where its high organic content and unusual speciation are burdensome for municipal wastewater resource recovery facilities (WRRF). Treating the aqueous phase adds undesirable cost to the HTL process, reducing its attractiveness. Here, we report aqueous phase supercritical upgrading (AP-SCU) as a new catalytic aqueous phase upgrading technology that reduces the organic content of the aqueous phase with co-production of supplemental biocrude. The supercritical phase provides sufficient catalyst activity for organic conversion, reduces energy inefficiency by eliminating the need for evaporation, and extends the catalyst lifetime relative to the liquid state. AP-SCU was evaluated at 380−440°C at 24 MPa for a representative HTL aqueous phase produced from the treatment of food waste. Using a ZSM-5 catalyst bound with silica sol, the aqueous carbon content was reduced by 64%−73% with a corresponding production of aromatic hydrocarbons including phenol and 2-pentanone. The total nitrogen was reduced by approximately 10%. Additionally, the ZSM-5 facilitated reduction and denitrogenation reactions of aqueous phase compounds to produce aromatic and pyridine compounds which more closely resemble HTL biocrude. After 3 h on stream, the catalyst experienced coke formation, and surface degradation which led to a reduction in acid sites and surface area. The carbon balance for the system was closed through the analysis of the aqueous, solid, and gas phases to estimate that biocrude yield varies from 43%−57% on a carbon basis. An energy balance for HTL process with integrated AP-SCU system showed that operating the AP-SCU unit at 380°C yielded the minimum energy demand for carbon removal at 63 MJ/kg-TOC. This value is greater than the energy demand for conventional WRRFs (37.9 MJ/kg-TOC) but is more than 10-times less than emerging technologies which are designed to handle complex feeds. AP-SCU

has potential as an energy efficient and effective new technology for reducing the TOC of the aqueous phase with simultaneous production of supplemental biocrude to offset energy demand.

1 Introduction

Solving the interconnected challenges of sustainable energy production and waste management is increasingly urgent, especially given that current projections predict a global population to exceed 9 billion people by the year 2050 (U. Nations, 2022). In the United States, approximately 292.4 million tons of municipal solid waste were generated in 2018, with only 35% being recycled or composted (EPA, 2022). Landfills are specifically problematic due to space limitations, potential for leachate runoff, and greenhouse gas emissions arising from anerobic digestion of landfill waste (Yaashikaa et al., 2022). Incineration, while reducing waste volume, can emit toxic substances such as dioxins and incineration of wet waste requires significant energy inputs, further prompting the search for more sustainable alternatives (Tait et al., 2020).

In response to these challenges, hydrothermal liquefaction (HTL) has emerged as a transformative technology for biomass conversion to fuels and chemical precursors (Beims et al., 2020). HTL operates under high temperature (typically 250°C–350°C) and pressure sufficient to maintain a liquid water phase, conditions which result in the efficient conversion of wet waste and lignocellulosic feedstocks—such as agricultural residues, municipal solid waste, and algal biomass—into an energy dense and carbon rich biocrude (LeClerc et al., 2022; Romano et al., 2023). The biocrude carbon yields have been shown to depend on both the lipid and solids contents of the feed, ranging in value from 39.7%–

74.3% (Cronin et al., 2022). Alternatively, carbohydrate and protein content mainly produce biocrude when they are present at a stoichiometric ratio appropriate for the Maillard reaction (Cronin et al., 2022). The HTL bio-crude can be further refined into a range of fuels and chemicals, thereby simultaneously reducing waste volumes and providing an inexpensive energy source and chemical feedstock (Usman et al., 2024).

In addition to the desired biocrude product, HTL generates char and gas byproducts and rejects some carbon to the water phase that exits the process (LeClerc et al., 2022). Efforts to characterize the fate of carbon in these auxiliary phases has shown that the aqueous phase yield can be predicted confidently alongside the biocrude based on the lipid content of the feed, while the solid and gas phases depend more strongly on process parameters than on feed characteristics (Cronin et al., 2022). For the HTL aqueous phase specifically, the organic content corresponds to a median chemical oxygen demand (COD), total organic carbon (TOC), and total nitrogen (TN) values of 25,000–75,000 ppm, 12,500–25,000 ppm, and 1,000–10,000 ppm depending on the feed (Watson et al., 2020). In principle, this carbon can be converted to methane via anaerobic digestion, an approach that is especially attractive for HTL treatment co-located at wastewater treatment plants. Unfortunately, compounds that interfere with anaerobic digestion are often present in the aqueous phase; for example, phenol concentrations have been reported to be in the range from 1,500–2,300 ppm, more than sufficient to disrupt anaerobic digestion (Sharma and Melkania, 2018). In addition to organic carbon, the aqueous phase contains

GRAPHICAL ABSTRACT
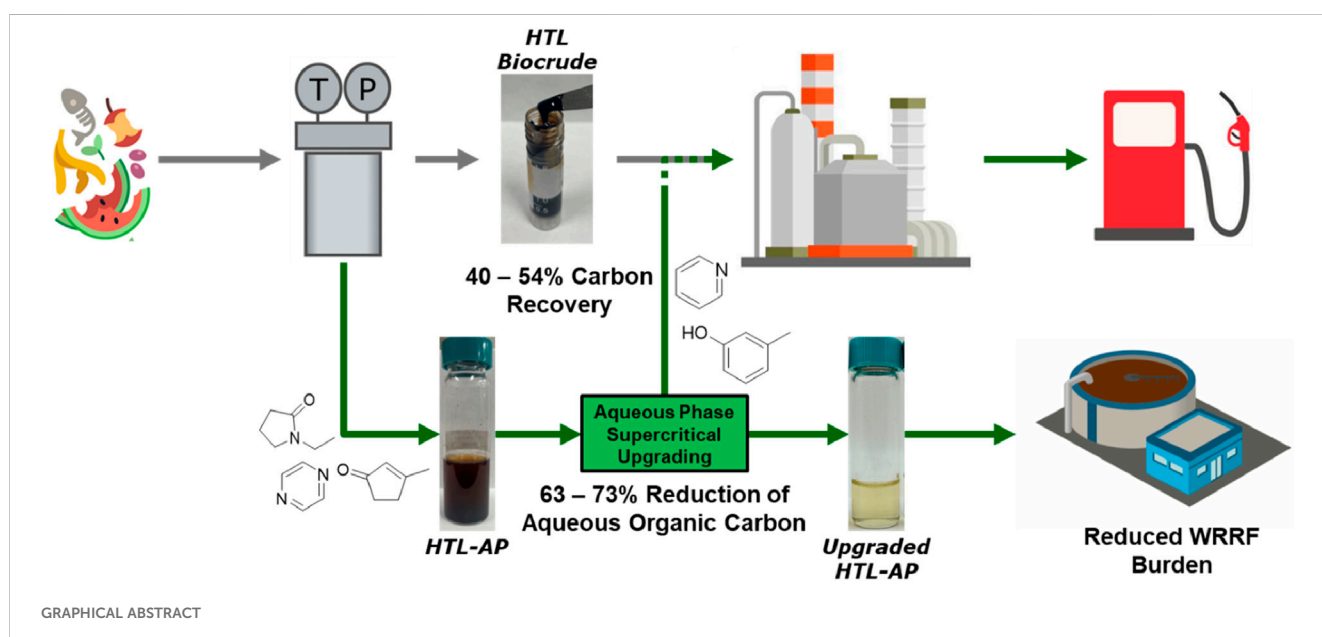
significant amounts of nitrogen in different forms, including ammonia (NH_3) (Yang et al., 2024). In high concentrations, nitrogen compounds can reduce the effectiveness of wastewater resource recovery facilities (WRRF) that use anaerobic digestion, reducing organic removal efficiency (Li et al., 2024). Not surprisingly, attempts to process HTL aqueous phases using anaerobic digestion have yielded mixed results (Zhu et al., 2023). Efforts to remove problematic nitrogen and phosphorous have been shown to be effective with membrane distillation and solvent extraction, however, these processes require harmful organic solvents and are also pH and temperature dependent and require further optimization (Rao et al., 2018). Gasification is an alternative valorization approach, but the high temperature it requires limits its thermodynamic efficiency (Swetha et al., 2021).

Instead of disposing of the aqueous phase as a waste stream, it has the potential to be valorized by converting its organic content into water insoluble products that can be used to boost biocrude yields while minimizing the influent TOC concentration for WRRFs. Of the existing technologies to valorize the hydrothermal liquefaction aqueous phase (HTL-AP), catalytic upgrading presents an opportunity to convert aqueous soluble compounds into energy-dense biofuel precursors such as aromatic hydrocarbons (He et al., 2018). Zeolites are a particularly attractive type of catalyst that can convert water soluble compounds present in the aqueous phase into water insoluble ones, such as benzene, toluene, ethyl benzene, and xylenes (BTEX) (He et al., 2018). For example, Page et al. observed rapid zeolite-catalyzed conversion of palmitic acid to BTEX and other one-ring aromatic compounds in the presence of liquid water (Page et al., 2022).

While the HTL-AP is rich in organics, its water content is typically around 95 wt%, which poses operational challenges. Performing the reaction in the vapor phase is the most desirable from the standpoint of catalyst stability, but evaporating the water phase makes vapor phase operation energetically unfavorable (Maag et al., 2019a). Alternatively, upgrading can be performed in the liquid state, as proposed recently by Maag et al. (2019a). In addition to avoiding evaporation, liquid phase upgrading confers energy balance and heat transfer benefits. On the other hand, liquid phase operation reduces catalyst stability compared with vapor phase operation. Most zeolites rapidly and irreversibly deactivate in the presence of liquid water (Maag et al., 2019b; Ravenelle et al., 2010; Zhang et al., 2015). Of the commercial options, ZSM-5 is widely regarded as the most tolerant of liquid water and in fact may be unusually stable at temperatures greater than the critical point of water (Maag et al., 2019b). The surprising water tolerance of ZSM-5 at temperatures above the critical point motivate its use for supercritical water upgrading of the HTL aqueous phase (Wang et al., 2020; Zaker et al., 2022). Catalytic upgrading of the HTL-AP in the presence of supercritical water therefore has potential to be an energy efficient and effective method of converting water soluble organic compounds into biocrude boosting molecules.

This study evaluates supercritical catalytic upgrading of an HTL aqueous phase using ZSM-5. The technology is termed aqueous phase supercritical upgrading (AP-SCU). A silica sol bound ZSM-5 was tested in a packed bed reactor to evaluate time-on-stream activity. An aqueous phase from HTL treatment of food waste was provided by PNNL as the feed for this process. The treated aqueous phase was collected at regular time intervals and analyzed

for total organic carbon, total nitrogen, as well as formation products that emphasize the potential for biocrude product formation. Used catalysts were studied to determine coke formation as well as signs of degradation. Mass and energy balances of the system highlight the potential for biocrude formation and recovery as well as for an efficient process for reducing TOC in complex wastewater solutions. These results validate supercritical water upgrading of the HTL aqueous phase as a new valorization method and suggest future studies to improve the technology.
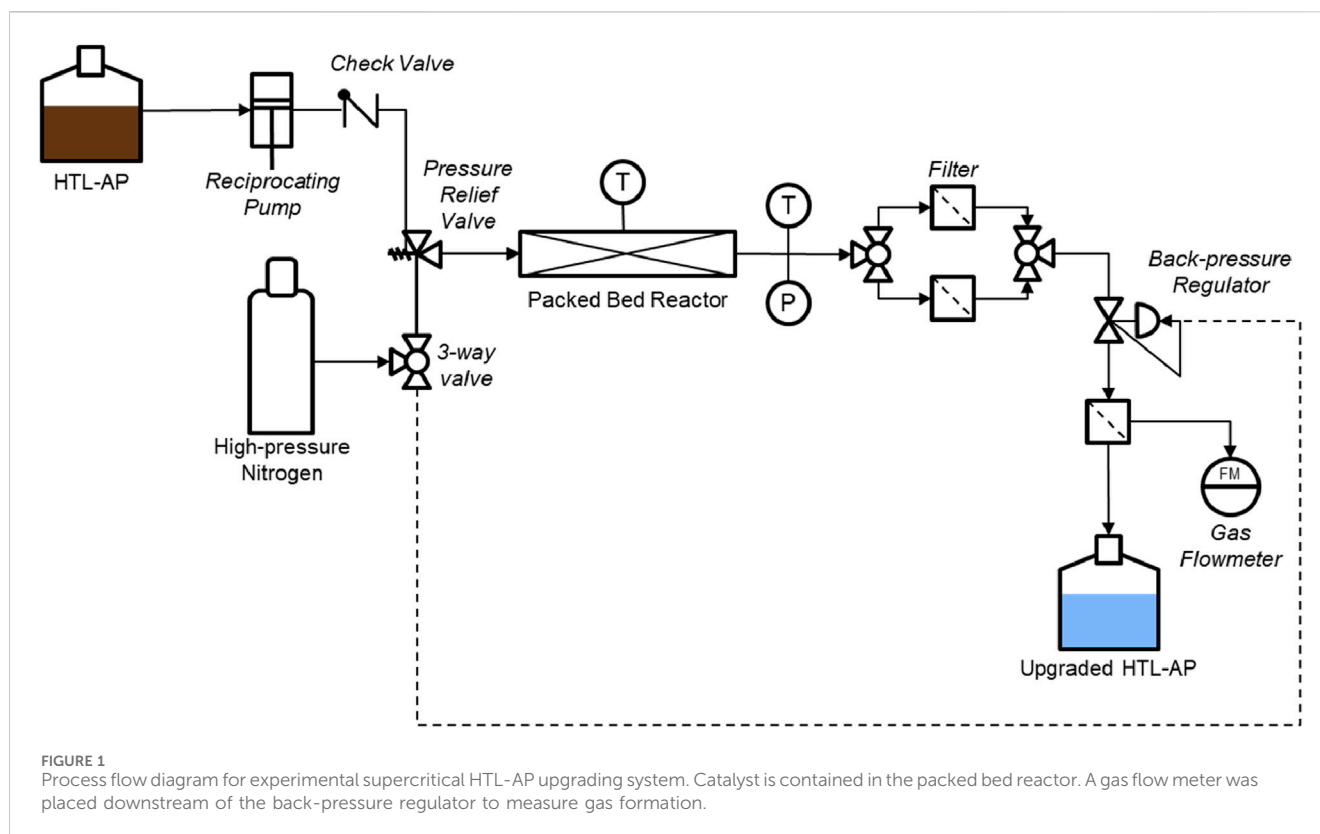
2 Methods

2.1 Materials

The hydrothermal liquefaction aqueous phase (HTL-AP) was provided by Pacific Northwest National Laboratory (PNNL). The HTL-AP was generated from an engineered bioslurry food waste (MHTLS-16, Supplementary Table S1) that was converted using PNNL's engineering-scale HTL flow system (Supplementary Figures S1–S2) (Snowden-Swan et al., 2022). The engineering-scale HTL system utilizes a plug flow reactor maintained at 350°C with a fluid residence time of 15 min. The solids, which are mostly inorganics, are removed at reaction temperatures and pressures. Removal of the solids enables a clean gravity separation of the HTL-AP from the biocrude in a conventional oil/water separator. More information on the HTL reactor system is described in the SI. For the specific experiment performed to generate the HTL-AP used in this study, the carbon yields of the biocrude, aqueous, gas, and solid phases were measured to be 69%, 19%, 9%, and 2%, respectively (Supplementary Table S2). Additional information on HTL product streams from food waste adjacent streams are provided in Supplementary Table S2. In addition to the analysis done by PNNL, the baseline values of the total organic carbon (TOC) and total nitrogen (TN) were measured using a Shimadzu TOC-L with the TN module. The TOC and TN were found to be 17,973 and 1,977 ppm, respectively.

The catalyst used in this study was a 40% ZSM-5 bound with silica solgel that was supplied by BASF Corporation. The material characterization showed that the particle size ranged from 96–104 μ m. Before using the catalyst, it was calcined to remove residual organics from its synthesis. Since ZSM-5 is known to be sensitive to water, including moisture in the air, the catalyst was first heated to 100°C for 1 h in air to evacuate all water from the oven. Next, the catalyst was calcined at 550°C in air for a minimum of 16 h.

2.2 Experimental design and operation

Prior to upgrading, the received HTL-AP was filtered to remove any remaining suspended solids to prevent clogging. The HTL-AP was cold centrifuged at −5°C for 3 h at 3,000 rpm to ensure that the mixture was completely separated. Once filtered, the HTL-AP was fed to a custom packed bed reactor (PBR) that was designed for this study (Figure 1). The system was constructed using 6″ of 1/4″ outer diameter Swagelok tubing. The packed bed reactor was loaded with 1.8 g of catalyst and then sealed. The reactor body was then encased in a heating block that was outfitted with a 500 W, 3/8″ x 8″

FIGURE 1
Process flow diagram for experimental supercritical HTL–AP upgrading system. Catalyst is contained in the packed bed reactor. A gas flow meter was placed downstream of the back-pressure regulator to measure gas formation.

cartridge heater purchased from McMaster Carr (4877K17, Supplementary Figure S3). Prior to heating, the reactor was pressurized to 24 MPa using high-pressure nitrogen that was supplied from Airgas (NI UHP300). Nitrogen was used to prevent the preloaded catalyst from being exposed to moisture from the air. Once pressurized, the heating block was set to the desired temperature (380°C–440°C). The temperature was controlled using a customized EZ Zone PID controller from Watlow with a k-type thermocouple purchased from Omega (KMQ316SS-062U-18). Once the internal temperature of the reactor reached the desired temperature, the HTL-AP was pumped through the reactor at a flowrate of 0.25 mL/min using a Knauer EPG HPLC pump (EPG20). Pressure was maintained using an Equilibar back pressure regulator (H6P) downstream of the reactor.

2.3 Sample collection and characterization

Once the internal liquid temperature reached the desired setpoint, the aqueous phase product was collected downstream of the backpressure regulator every 30 min for 3 h. Gas phase flow rates were measured periodically. The sensitivity of the gas phase flow meter was 1 mL/min. Since no gas phase was ever detected it was implied that the maximum yield of gas phase was less than 1 mL/min. After collecting the sixth sample, the run was concluded, the fluid flow was suspended, and the heater was turned off. The system was depressurized once the system reached 70°C to prevent rapid evaporation. Once at atmospheric pressure, the remaining HTL-AP was purged from the system with more high-pressure nitrogen. The

spent catalyst was then extracted for post-run analysis while the residual biocrude was washed out of the reactor with solvents.

The change in total organic carbon (TOC) and total nitrogen (TN) of the recovered HTL-AP was analyzed by diluting 15 μl to 100 mL and analyzed on a Shimadzu TOC-L with TN module. To identify aqueous soluble reaction products, the recovered aqueous phase was mixed with dichloromethane (DCM) in a 1:1 volume ratio to maximize solute partitioning into the solvent phase. The saturated solvent was then analyzed using a Shimadzu GC-MS.

The post reaction catalyst was analyzed using a Rigaku Geigerflex XRD both before and after calcining to remove organic residues. Additionally, the catalysts were imaged before and after the reaction using a JEOL FE-SEM to identify potential degradation in the ZSM-5 structure. For quantitative analysis, catalyst samples were analyzed for coke formation using thermogravimetric analysis, surface area using gas sorption, and acid site density using Fourier Transform Infrared Spectroscopy. More information on catalyst analysis methodology is provided in the SI.

2.4 Mass and energy balances

In a typical run, approximately 50 mL of aqueous phase were processed. The theoretical biocrude yield is 1 g for every 50 mL of aqueous phase processed. Approximately 50% of the theoretical yield was achieved and the biocrude produced during a run phase separated in the quench section and entered into dead spots in the tubing without exiting the experimental apparatus. This made direct biocrude yield quantification inaccurate. Instead, the biocrude yield

was estimated using mass balance consideration, in which the carbon yield of biocrude ($m_{C,biocrude}$) equaled the carbon that entered the reactor less the carbon yield in the aqueous, solid, and gas phases (Equation 1).

$$m_{C,biocrude} = m_{C_{in}} - \left[m_{C,aq} + m_{C,gas} + m_{C,solid} \right] \qquad (1)$$

For this balance, $m_{C,aq}$ is the total aqueous phase carbon that remains in the aqueous phase after passing through the reactor (Equation 2):

$$m_{C,aq} = \sum_{i=1}^{6} [TOC] \cdot V_i \qquad (2)$$

$m_{C,aq}$ is represented as a summation across i samplings of the reactor system. Since the system was sampled every 30 min across a 3-hour period, there are a total of 6 samples. For each sample, the total carbon recovered in the aqueous phase is the product of the total organic carbon concentration ($[TOC]$) [ppm], and the volume of the recovered sample (V_i) [L]. $m_{C,gas}$ is the carbon present in the formed gas product. Gas flow measurements indicated a maximum gas product flow rate of 1 mL/min. Based on previous studies, the composition of the gas mixture was assumed to be a mixture of carbon dioxide (CO_2), carbon monoxide (CO), and methane (CH_4) in a 92:7.4:0.6 ratio. (Ellersdorfer, 2020) Therefore, $m_{C,gas}$ was calculated with Equation 3:

$$m_{C,gas} = \left(\left(0.92 \cdot \rho_{CO_2} \cdot \left(\frac{MW_C}{MW_{CO_2}} \right) \right) + \left(0.074 \cdot \rho_{CO_2} \cdot \left(\frac{MW_C}{MW_{CO}} \right) \right) \right.$$
$$\left. + \left(0.006 \cdot \rho_{CH_4} \cdot \left(\frac{MW_C}{MW_{CH_4}} \right) \right) \right) \cdot t \qquad (3)$$

where ρ is the gas phase density [g/mL], MW is the molar mass [g/mol], and t is the total reaction time [min]. Lastly, $m_{C,solid}$ was estimated using the mass of coke measured on the used catalyst. The thermogravimetric analysis (TGA) of the spent catalyst samples were included contributions from carbon, nitrogen, and sulfur containing species, so it is assumed that 96% of the coke is carbon, based on previous hydrocarbon upgrading studies with similar operating conditions. (Karge et al., 1991) The $m_{C,solid}$ can then be estimated using Equation 4:

$$m_{C,solid} = 0.96 \cdot m_{catalyst} \cdot R \qquad (4)$$

where $m_{catalyst}$ is the mass of the recovered catalyst [g], and R is the percent of residual coke identified on the catalyst [%].

The energy demand of the process was calculated as the energy required to heat the system to the operating condition, normalized to the mass of organic carbon that was removed from the system (Equation 5):

$$E = \frac{\Delta H \cdot \rho \cdot V}{m_{C_{in}} - m_{C_{aq}}} \qquad (5)$$

In Equation 5 E is the total energy input [MJ/kg-TOC], ΔH is the change in fluid enthalpy due to heating as provided by NIST [MJ/kg], ρ is the fluid density [kg/L], V is the volume of fluid that was managed [L], and $m_{C_{in}}$ and $m_{C_{aq}}$ are the inlet and outlet organic carbon values [kg-TOC]. Heat recovery was modeled as ideal counter-current heat exchangers.
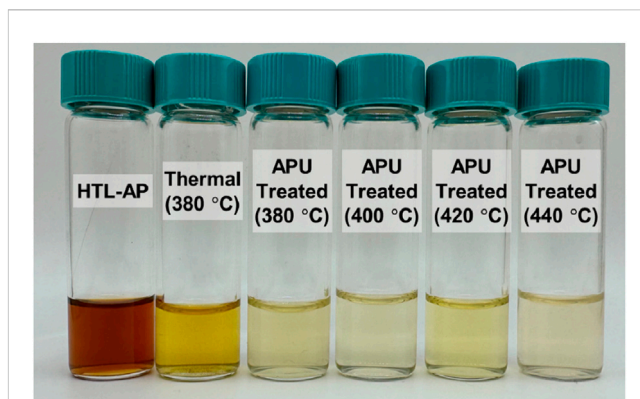

FIGURE 2
Images of the HTL aqueous phase that has been collected within the first 30-minute sampling window. From left to right: HTL-AP, thermally upgraded, AP-SCU at 380°C, 400°C, 420°C, and 440°C. Each sample was filtered to remove suspended particulates.
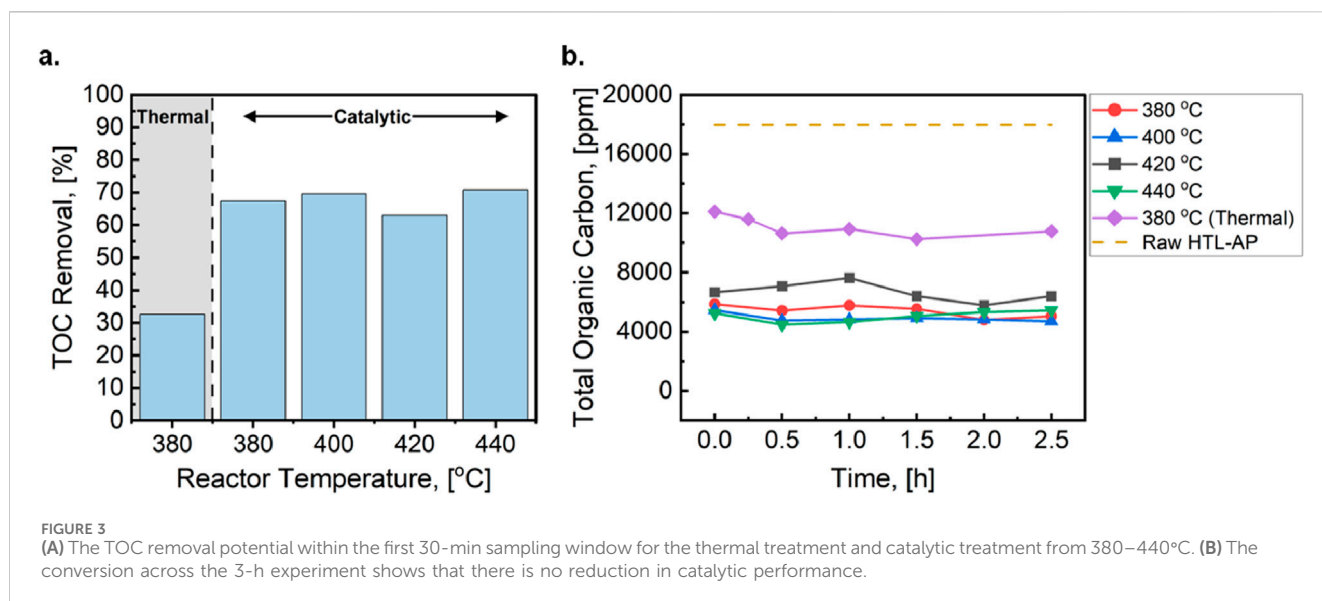
3 Results and discussion

Experiments were performed in the continuous-flow packed bed reactor in the absence of catalyst at 380°C, termed "thermal conditions" and used as a benchmark, and in the presence catalyst at 20°C intervals from 380°C to 440°C. Aqueous phase samples were analyzed for TOC and TN reduction, the catalyst was recovered and characterized for evidence of degradation, and mass and energy balances were performed to determine the energy efficiency of the TOC reduction.

3.1 Temperature effect on the fate of carbon

The most important goal of this work is the reduction of total organic carbon (TOC) in the HTL-AP. Accordingly, the post-reaction aqueous phase was collected and imaged, highlighting a significant change in visual appearance (Figure 2). Specifically, the raw HTL-AP is a dark amber color, an indicator of a relatively high concentration of dissolved organic carbon. A control test consisting of thermal treatment of the HTL-AP at 380°C without catalyst results in a dark yellow product mixture, indicating that heating without a catalyst has minimal effect on the HTL-AP. Treatment with ZSM-5 catalyst changes the HTL-AP color to pale straw, completely translucent, and nearly transparent. The visual difference in the treated product compared with the feed is qualitative evidence of a reduction in carbon content and change in composition.

Figure 3 provides quantitative TOC removal measured for AP-SCU as a function of temperature and time-on-stream at constant reactor space velocity. Under catalytic conditions, the TOC concentration was reduced by 63%–71% during the first 30-min sampling period (Figure 3A). As a control, AP-SCU was performed without the ZSM-5 catalyst to deconvolute the TOC reduction potential of the catalyst and elevated temperature. Figure 3A shows that the thermal treatment could only reduce the TOC concentration by 33%. This indicates incorporating the ZSM-5 catalyst provides a 2-fold increase in removal potential for

FIGURE 3
(A) The TOC removal potential within the first 30-min sampling window for the thermal treatment and catalytic treatment from 380−440°C. **(B)** The conversion across the 3-h experiment shows that there is no reduction in catalytic performance.

dissolved organics. After the first 30-min sampling window, Figure 3B shows the TOC concentrations as a function of time-on-stream and at different reaction temperatures for both the control and catalytic tests. TOC removal was consistent for the 3-hour testing period, indicating stable catalyst performance for the duration of the experiment.

With an insufficient biocrude yield expected during these experiments, identifying the production of partitioning organic carbon compounds with GC-MS was performed as an alternative to biocrude analysis to provide insights into the reactions taking place during catalytic upgrading. Results from GC-MS analysis the HTL-AP feed and treated products are provided in Figure 4. The HTL-AP fed to the reactor contains many GC-analyzable compounds, with the primary classes including pyrazines, as well as cyclic and aromatic hydrocarbons. Figure 4 indicates that the speciation of aqueous compounds resulting from the AP-SCU are similar regardless of the operating temperature which is consistent with the observation made in Figure 3 that the AP-SCU performance is weakly dependent on temperature. Overall, the total peak area of GC-analyzable compounds decreases after AP-SCU treatment, which is consistent with the ~70% decrease in TOC shown in Figure 3A. Further, the AP-SCU product mixture contains an increased abundance of pyridines and aromatic hydrocarbons relative to the feed. Relative to the HTL-AP feed, the aromatic content of the product stream is increased by a factor of 10. This observation indicates that aromatization reactions produce these compounds, a mechanism frequently reported for ZSM-5 zeolites due to the Brønsted acidity and steric selectivity of the MFI channels (Xin et al., 2014; Lok et al., 2019). Production of aromatic compounds during AP-SCU adds a valuable product stream that can offset operational costs of the treatment. A complete list of GC-identifiable compounds as well as the concentration of the three primary products within the solvent phase are listed in Supplementary Table S3 and Supplementary Table S4. The inset plot in Figure 4B provides time-on-stream product composition data, showing that the production of aromatic hydrocarbons remains constant over the 3-hour operation window for the AP-

SCU process and reinforcing the potential for catalyst longevity. Unlike TOC reduction, aromatic yields increase modestly with increasing reaction temperature, with a 50% increase observed between 380°C and 440°C. Accordingly, while TOC reduction recommends operation at 380°C (or lower, if feasible), co-product yields benefit from higher temperature operation.

3.2 Fate of total nitrogen

The MHTLS-16 feed used in this study had a nitrogen content of 3% (Supplementary Table S1), consisting of both organic and inorganic (NO_3^-, NO_2^-, NH_4^+) nitrogen. The received HTL-AP was found to have a total nitrogen content of 1,977 ppm. Reducing this nitrogen content is required either for discharge or prior to sending the aqueous phase to water treatment. AP-SCU will convert some fractions of the organic nitrogen into oil-soluble compounds, with deep denitrogenation being especially desirable since nitrogen content of fuels is strictly regulated. Figure 5 shows time-on-stream measurements of total nitrogen (TN) concentration of the upgraded HTL-AP under thermal conditions and in the presence of catalyst at temperatures from 380°C to 440°C. The TN content of the HTL-AP is shown for reference. Interestingly, thermal processing increases the TN content of the aqueous phase, likely due to partial evaporation of water during processing, resulting in a concentrating effect for residual nitrogen relative to the HTL-AP as received. In comparison, AP-SCU reduces the TN content by 9%, with consistent performance as a function of time-on-stream up to 3 h and over the entire temperature range considered in this study. Reduction of TN by 9% is likely attributable to a combination of organonitrogen compound destruction and removal by partitioning of newly produced aqueous-insoluble organic compounds; however, this is assumed to be close to the limit that can be achieved by this technology, since NH_3 and nitrate are unreactive. Figure 5 therefore places an upper bound on the potential for AP-SCU; it is an effective technology for modest reduction in organic nitrogen content of the aqueous phase but should not be considered for complete organic
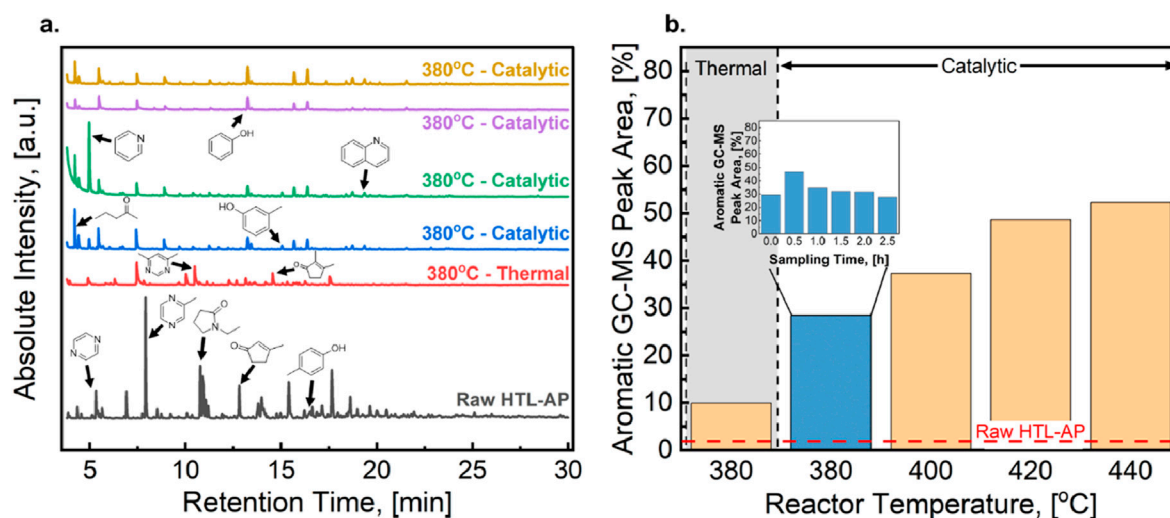
FIGURE 4
(A) GC-MS chromatogram of the HTL-AP before and after the initial 30-min sampling window in the presence of ZSM-5. The compounds highlighted are representative structures for the most abundant compounds identified within the aqueous phase. **(B)** GC-MS peak area of hydrocarbon aromatic compounds within the initial 30-minute sampling window under each operating condition. The peak area was normalized to the area of all identifiable compounds. Inlaid in the plot is the GC-MS peak areas for hydrocarbon aromatic compounds at 380°C along the 3-hour sampling window.
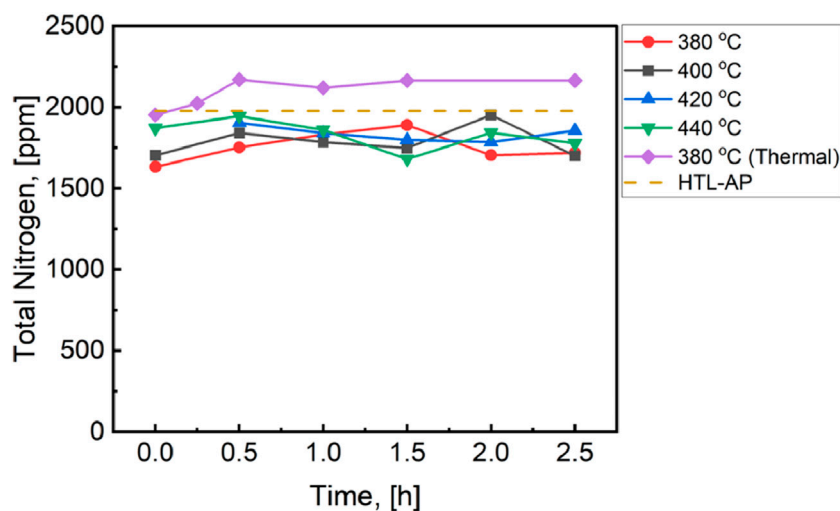

FIGURE 5
Averaged total nitrogen for the HTL-AP for each of the reaction conditions. The slight reduction in TN for the upgraded aqueous phases likely points to the overwhelming presence of inorganic nitrogen.

nitrogen removal nor for NH_3 and nitrate removal. Fortunately, both NH_3 and nitrate can be recovered using existing technologies and both substances have many applications, including as a soil amendment in agriculture.

The GC-MS data that was presented in Figure 4A provides information on organic nitrogen abundance in the AP-SCU product. Figure 6 uses GC-MS peak areas to estimate the abundance of compounds identified as pyrazines, pyridines, and as other nitrogen-based compounds. In the HTL-AP feed, 3% of the peak area is identified as pyridine, 20% as other nitrogen-based compounds, and 34% as pyrazine. After AP-

SCU treatment, the only identifiable nitrogen-containing compound class is pyridine. The clear shift in pyridine selectivity after AP-SCU relative to the pyrazines present in the HTL-AP could be attributed to chemical reactions such as dehydration of cyclic nitrogen species such as pyrrolidine, or a denitrogenating of pyrazine compounds to form pyridines. Another explanation could be a selective catalyst adsorption and reaction of pyrazines with two nitrogen atoms within the aromatic ring, which has been suggested to be distinct from the adsorption behavior of pyridines on zeolite. (Tam and Cooney, 1976).
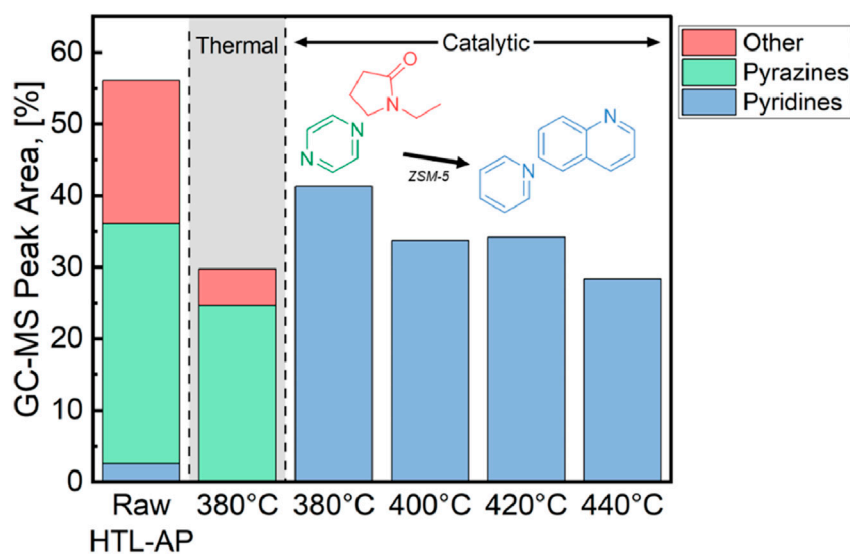
FIGURE 6
GC-MS peak area of nitrogen containing compounds within the initial 30-minute sampling window under each operating condition. The peak area was normalized to the area of all identifiable compounds.

Figure 6 helps reconcile the modest TN reductions reported in Figure 5. Not only are nitrate and NH_3 inert under these reaction conditions, but also pyridine is a stable end product of its own. Channeling the organic nitrogen content into a single category is extremely beneficial for attempts at cleanup or valorization that may occur downstream of AP-SCU. In particular, pyrazines have broad herbicidal properties which could inhibit crop growth, therefore preventing HTL-AP from being used as a fertilizer (Doležal and Kráľová, 2011). In comparison, pyridine has much more targeted herbicidal properties, especially for broad-leaf weeds (EPA, 2024). Accordingly, after AP-SCU treatment, the treated aqueous phase may prove to be much more useful for agricultural purposes than the original HTL-AP.

3.3 Used catalyst characterization

Organic carbon, total nitrogen, and molecular analysis indicate that the supercritical water upgrading technology has potential for converting rejected carbon present in the HTL aqueous phase into useful products. Catalyst stability at timescales relevant for industrial use is also required in addition to the previously shown performance. Catalyst stability can be evaluated based on three metrics: 1) deactivation of catalyst due to coke build-up on the external surfaces and within pores, 2) selective loss of acid sites from zeolite framework and 3) loss of bulk zeolite crystallinity resulting in an amorphized residue. Each of these metrics was evaluated to gain insight into catalyst deactivation.

Photographs of the catalyzed recovered after use for AP-SCU (Figure 7) show that the material is transformed from a uniformly sized white powder to a blackened agglomerate indicative of coking. Coking had negligible impact on the apparent catalytic activity after 3 h of AP-SCU under all operating temperatures, based on the time-on-stream data shown in Figures 3, 5. Coke content ranged from

3–6.4 wt% (Supplementary Table S5). The production of coke without a loss in catalytic activity is attributable to either active sites primarily near the surface or pore blockage from coke accumulation over the observed 3-h sampling time. TGA analysis indicated that the coke was a combination of carbon, nitrogen, and sulfur containing species. The sulfur and especially nitrogen content of the feed may promote coking since basic nitrogen compounds will bind to catalytically active sites and deactivate them. Removing the aqueous samples of inorganic nitrogen and sulfur such as ammonia (NH_3), nitrate (NO_3^-) and sulfate (SO_4^{2-}) may likely reduce the initial deactivation of acid sites present in the catalyst.

Framework crystallinity was characterized by comparing the x-ray diffractograms (XRD) of fresh and catalysts used for 3 h time-on-stream tests under AP-SCU conditions, as shown in Figure 8. The calcined ZSM-5 catalyst has peaks consistent with ZSM-5, particularly the peaks between 5–7 2θ degrees, as well as the prominent peak at 22.5 2θ degrees. Other observed peaks can be attributed to the catalyst substrate. After AP-SCU at 400°C, the intensities of peaks associated with ZSM-5 have decreased, with the appearance of new characteristic peaks associated with the formation of alumina, sodalite and coke. Compared with the sample obtained after AP-SCU at 400°C, the intensities of alumina, sodalite, and coke peaks are more pronounced in the catalyst used for AP-SCU at 440°C. These observations indicate partial degradation of ZSM-5 during AP-SCU (Maag et al., 2019b). Degradation of the ZSM-5 was confirmed through a similar loss of SiO_2 support at all reaction temperatures and ranging from 13% to 24% (Supplementary Table S6) as well as an average decrease of 81% in surface area for the spent catalysts in comparison with the fresh catalyst (Supplementary Table S7). In addition to surface area losses, Brønsted acid density (Supplementary Table S8) decreased by as much as 99.8% following use. While there is a near complete depletion of Brønsted acid sites, Lewis acid density increased for catalysts used at 380–420°C, which may explain apparent retention
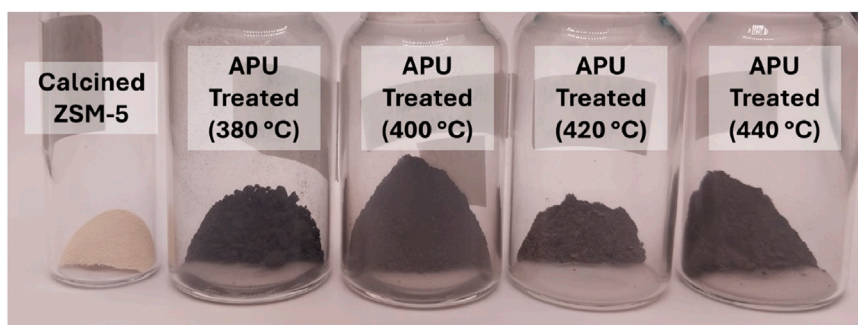
FIGURE 7
Image of calcined ZSM-5 catalyst prior to and after AP-SCU treatment temperatures of 380, 400, 420°C and 440°C.
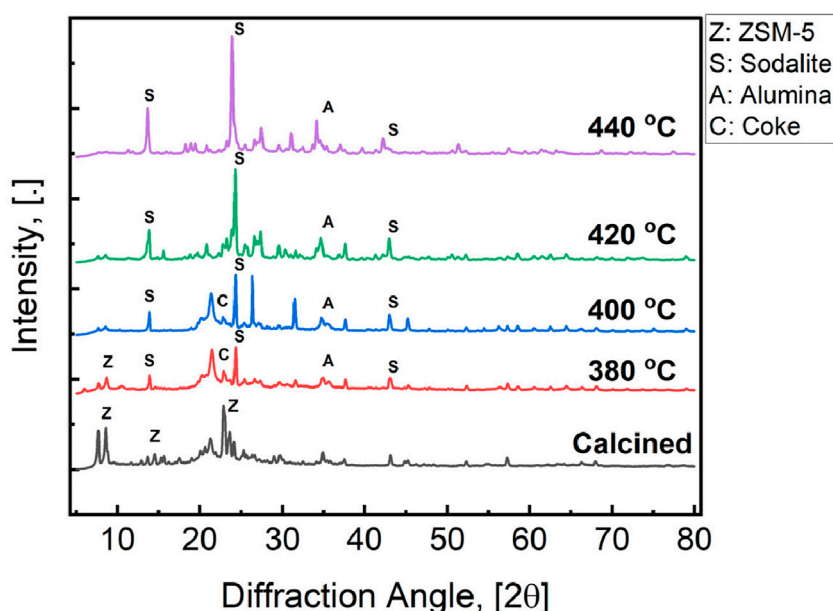

FIGURE 8
XRD diffraction patterns of the ZSM-5 catalyst before and after treatment at 380°C, 400°C, 420°C, and 440°C.

of activity and opening potential opportunities for replacing ZSM-5 with lower cost (or more stable and more active) catalysts.

XRD identification of sodalite in the used catalyst merits further consideration. Previous studies that have evaluated ZSM-5 degradation in hot liquid water (HLW) did not observe the formation of sodalite, although other studies have shown recrystallization into other frameworks after prolonged treatments (Jamil et al., 2016). While amorphous silica produced from ZSM-5 degradation could eventually recrystallize, the presence of sodalite cages after AP-SCU treatment does not prove a preferential recrystallization since it is also one of ZSM-5 several building blocks (McCusker et al., 2005). The observation of sodalite in XRD is consistent with either their relative hydrothermal stability and/or ability to seed growth of sodalite cages under AP-SCU conditions. Further studies are required to understand the decrystallization of ZSM-5 and potential for sodalite growth under AP-SCU conditions.

Scanning electron micrographs provided in Figure 9 aid in understanding shifts in ZSM-5 crystal morphology and surface degradation during AP-SCU treatment. The original catalyst (pictured in Figure 9A) consists of micron-sized ZSM-5 crystals. The ZSM-5 crystals are uniformly distributed across the microspherical particle and the surface of the particle exhibits minimal-surface roughness. After AP-SCU treatment, morphological shifts are observed that can be attributed to a combination of coke and zeolite removal. After AP-SCU treatment at 380°C, the underlying spherical substrate is retained, however, the zeolite distribution is no longer uniform based on the increased surface roughness shown in the lower magnification. Furthermore, the increased magnification image reveals a crystal structure that appears both larger in size and delaminated when compared with the ZSM-5 crystals present on the fresh catalyst. Larger crystal sizes are consistent with zeolite aggregation and the crystal morphology change suggests surface degradation in the form
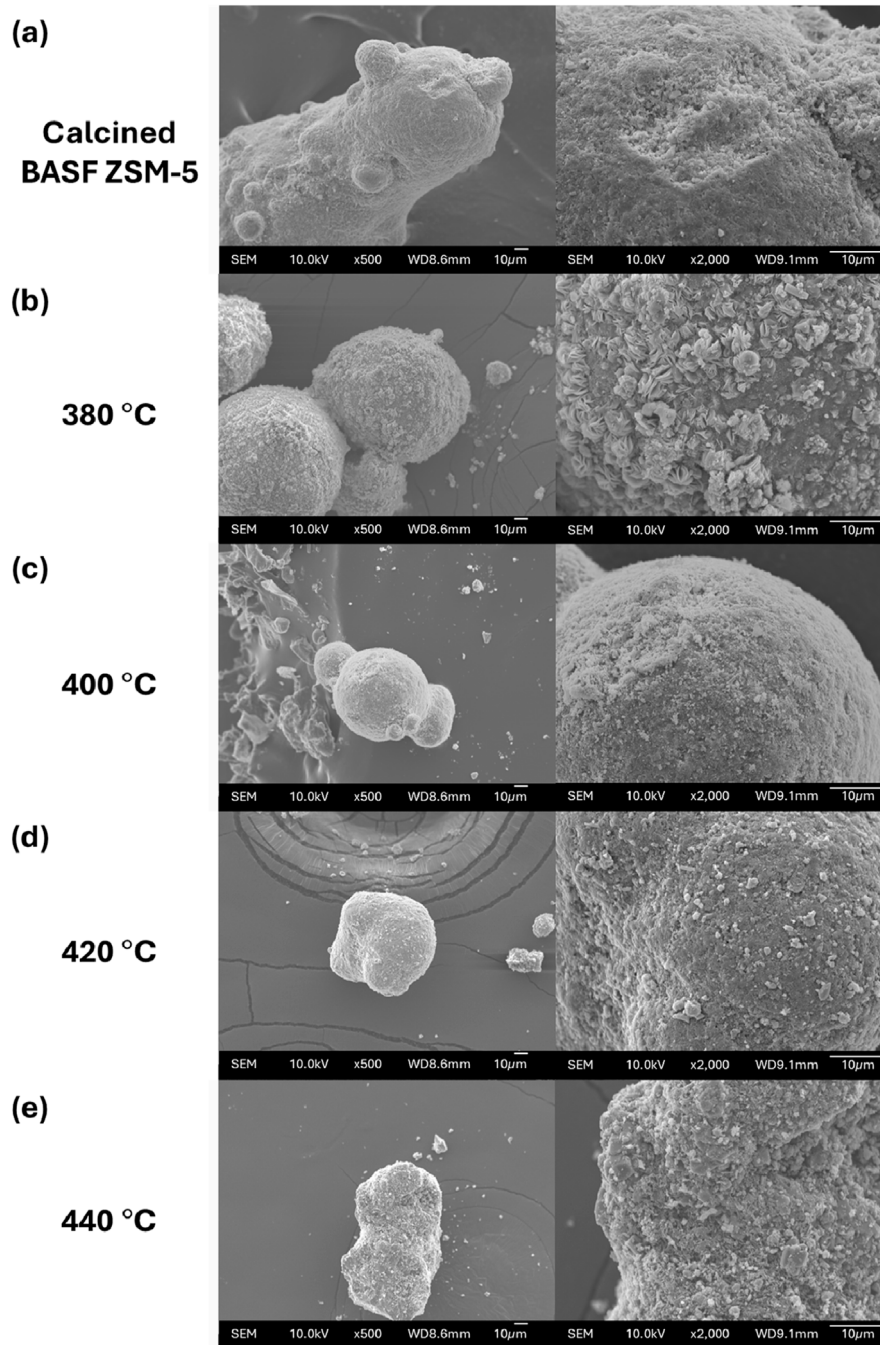
FIGURE 9
SEM images of the catalyst **(A)** as received and after AP-SCU at **(B)** 380°C, **(C)** 400°C, **(D)** 420°C, and **(E)** 440°C.

of zeolite desilication. Increased surface roughness has been previously shown for zeolites treated under HLW conditions (Maag et al., 2019b; Ravenelle et al., 2010). Similar retention of the substrate structure is observed at elevated AP-SCU operating temperatures of 400°C–440°C shown in the low magnification images (Figures 9C–E). However, the substrate surface is progressively less populated with zeolite crystals when samples are recovered after AP-SCU at increasing temperature. Furthermore, smooth agglomerates of varying size and shape are present on the substrates treated under AP-SCU conditions >380°C

and the observed delaminated zeolite shown are no longer apparent. The contrast between zeolite crystal morphology and abundance found after AP-SCU temperatures ≤380°C compared to >380°C aligns with the unique shift in thermophysical properties of water near supercritical condition; namely, the ability to contain reactive ions for zeolite decrystallization drastically decreases under supercritical compared to subcritical or near-critical water (Armellini and Tester, 1993). Despite the drastic change in observed zeolite crystal morphology, the retained activity suggests that a combination of the retained zeolite and/or substrate is
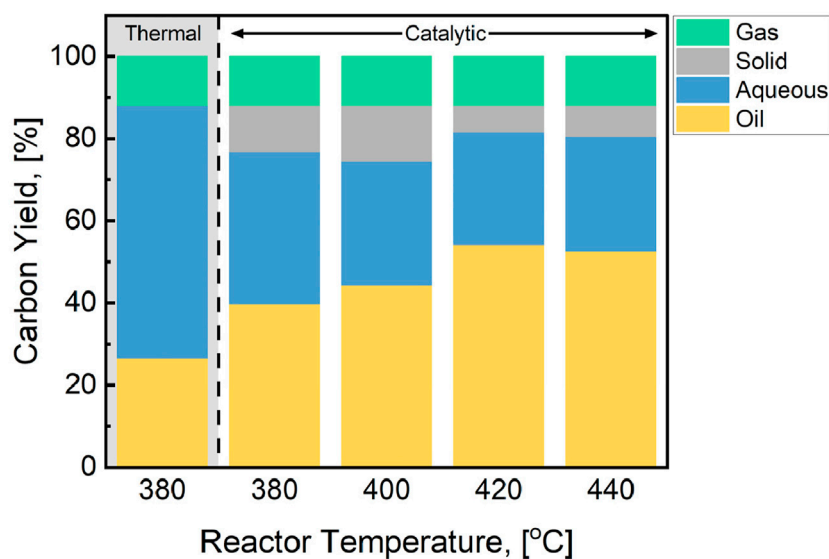
FIGURE 10
Carbon balance for the AP-SCU system for all operating conditions.

providing sufficient active sites to aromatize and condense aqueous phase organics under high conversion conditions and that activity is retained after 3 h of AP-SCU treatment.

3.4 Mass and energy balance analysis

AP-SCU aims to reduce the organic content of the HTL aqueous phase to reduce the burden on wastewater treatment while producing a biocrude product to offset energy requirements. An important consideration is energy requirements relative to the TOC reduction. Accordingly, mass and energy balances were used to estimate biocrude yields and energy inputs.

Biocrude quantities generated over the duration of an entire experiment were insufficient (<1 g) for direct quantification as these small quantities tended to accumulate in irremovable stagnation spots in the cool-down section downstream of the packed bed reactor. Instead, mass balance, as shown in Equation 1, was used to estimate biocrude carbon yields. The results are summarized in Figure 10, which shows that a maximum of about 50% carbon yield as biocrude could be obtained at 420°C and 440°C. Use of ZSM-5 catalyst nearly doubles biocrude yield compared with thermal reaction at the same temperature. Increasing temperature under catalytic conditions corresponds to increased biocrude yield up to 420°C. Above 420°C, rapid catalyst deactivation likely contributes to diminishing returns in terms of increased biocrude yield with increasing reaction temperature.

Next, the energy balance for this system was benchmarked against traditional HTL, using the process flow diagram shown schematically in Figure 11. The first scenario (Figure 11A) represents a simple HTL flow system where the reactor operates at 350°C and the incoming feed is preheated with the outgoing reaction products using a counter current heat exchanger. The proposed system (Figure 11B), which integrates HTL with the AP-SCU reactor, is composed of an HTL reactor operating at

350°C, with downstream cooling of the HTL reaction products to 300°C, an intermediate temperature selected based on the minimal solubility of key biocrude components such as fatty acids at this condition (Briones et al., 1989). After biocrude-aqueous phase separation, the aqueous phase is then heated back to the desired AP-SCU temperature (380–440°C) for TOC reduction and additional biocrude production. The heating value of the additional biocrude produced from the HTL-AP is used to partially offset the energy demand required to heat to AP-SCU conditions. The reaction products from the AP-SCU preheat the incoming waste slurry prior to entering the HTL reactor system. Heat exchange cannot heat the incoming feed to HTL temperature; to account for the makeup heat ($\dot{Q}$), is added as needed. Sample calculations for the energy balance can be found in the SI.

Table 1 provides key results of the energy balance, specifically, the additional energy required to operate the integrated process compared with HTL on its own, the amount of biocrude produced in order to reduce each kg of TOC, and the corresponding energy required to remove aqueous TOC under each operating condition. For most conditions, the AP-SCU system requires more energy than the stand alone HTL system, but 380°C requires less energy than a standalone HTL unit. For the other conditions, a careful use of heat recovery will maintain the difference in energy demand to 0.1–0.2 MJ/kg-H_2O. Figure 10 indicates that 420°C achieves a local optimum for oil production, however, when accounting for the total carbon removed from the aqueous phase Table 1 shows that the overall energy to remove TOC from the HTL-AP ranges from 63–76 MJ per kg of TOC, with 380 °C being the optimal condition. For comparison, thermally upgrading at the same temperature requires nearly double the energy per kilogram of removed organic carbon than the catalytic process.

Benchmarking the values in Table 1 against alternative technologies provides valuable context. WRRFs receive inflows with TOC concentrations ranging from 100–200 ppm, achieving up to 95% reduction before discharging (Law et al., 2013; Welsh, 2024). A typical energy demand to achieve this TOC reduction by a
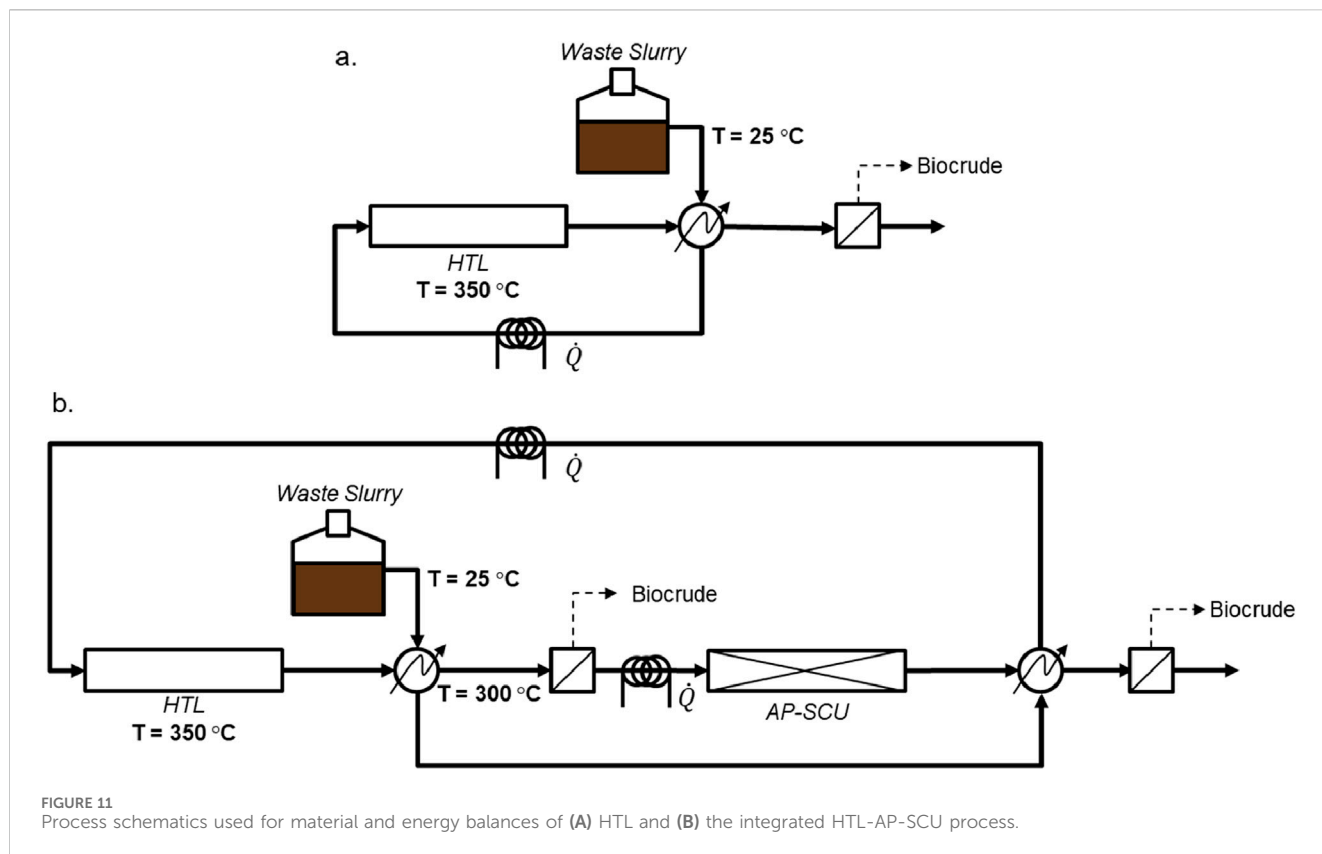
FIGURE 11
Process schematics used for material and energy balances of **(A)** HTL and **(B)** the integrated HTL-AP-SCU process.

TABLE 1 Calculated energy demands for HTL as well as the integrated AP-SCU systems.

Scenario	Net system energy demand (MJ/kg-H$_2$O)	Ratio of biocrude to aqueous TOC (kg/kg)	Additional TOC removal (MJ/kg-TOC)
HTL	0.8	3.4	-
APU – 380ºC (Thermal)	0.8	6.8	119
APU – 380ºC	0.7	11.9	63
APU – 400ºC	0.9	14.9	75
APU – 420ºC	0.9	16.9	70
APU – 440ºC	1.0	16.4	76

TABLE 2 Energy demands for emerging wastewater treatment technologies aimed at handling complex and toxic feeds.

Technology	Energy demand (MJ/kg-TOC)	References
Dual Plasma Discharge System	936	Saleem et al. (2025)
Electrochemical Oxidation	1,080	Valenzuela et al. (2017)
Electrocatalysis	2,880	Santos et al. (2020)

WRRF is 37.9 MJ/kg TOC (Hamawand, 2023). AP-SCU is therefore less energy efficient than standard WRRF technology. That stated, the HTL-AP cannot be recycled to the WRRF inlet stream, due to toxicity effects (Watson et al., 2020). Accordingly, emerging technologies that are compatible with treatment of toxic mixtures are a more realistic comparison for the energy requirement of HTL-AP. Table 2 provides energy input values for several emerging technologies, including plasma treatment and electrochemical treatments. The energy demands of several promising emerging technologies are at least 10x greater than that estimated for HTL-AP.

Accordingly, AP-SCU provides a much more energy efficient method of reducing the TOC content of the HTL-AP than other emerging, toxic-substances-tolerant technologies currently under consideration. Co-production of biocrude plays an important role in the energy efficiency of AP-SCU, as does careful process design.

4 Conclusion

Hydrothermal liquefaction aqueous phase (HTL-AP) is a source of organic carbon that can be valorized as chemical and fuel products, thereby adding a new value stream to an HTL process and reducing the burden on downstream cleanup. In this study, aqueous phase supercritical upgrading (AP-SCU) was evaluated as a new, catalytic supercritical water technology for energy efficient conversion of water-soluble compounds present in the aqueous phase into useful chemicals, while simultaneously reducing its organic content. Supercritical conditions support the upgrading of the aqueous phase in two ways: (1) eliminating the need for vaporizing the aqueous phase, a process which is energy intensive due to the latent heat of vaporization, and (2) reducing degradation of low-cost zeolite catalysts relative to that expected in a liquid phase, and thereby increasing overall performance. Silica sol bound ZSM-5 was used as the catalyst in time-on-stream tests at temperatures from 380°C to 440°C at 24 MPa. Reductions in organic carbon (70%) and total nitrogen (10%) were found to be insensitive to temperatures. Characteristic zeolite reactions, like the formation of aromatic hydrocarbons and changes in speciation of organic nitrogen, were observed at all conditions. Nitrogen compounds were channeled into a single class of compounds, pyridines, making subsequent polishing or valorization of the treated HTL-AP easier than the original. Stable TOC reduction was observed over the entire 3-h sampling window that was tested, despite catalyst degradation revealed by post-use characterization. Mass and energy balances indicated that the catalytic process is much more efficient than thermal processing and 10x more efficient at reducing TOC than other emerging methods capable of handling toxic compound mixtures. AP-SCU offers a new, potentially energy efficient method for reducing the TOC content of HTL-AP, while simultaneously producing an energy rich biocrude supplement. Future work will focus on replacing the catalyst support to extend material stability.

Data availability statement

The raw data supporting the conclusions of this article will be made available by the authors, without undue reservation.

Author contributions

DK: Data curation, Formal Analysis, Investigation, Validation, Visualization, Writing–original draft, Writing–review and editing. AM: Conceptualization, Data curation, Formal Analysis, Investigation, Methodology, Visualization, Writing–original draft. OS: Conceptualization, Data curation, Formal Analysis, Investigation, Methodology, Visualization, Writing–original draft. JY: Conceptualization, Data curation, Formal Analysis, Investigation, Methodology, Visualization, Writing–original draft. CK: Data curation, Formal Analysis, Resources, Writing–original draft, Writing–review and editing. AS: Data curation, Formal Analysis, Methodology, Resources, Writing–original draft, Writing–review and editing. GT: Conceptualization, Data curation, Formal Analysis, Investigation, Methodology, Project administration, Resources, Supervision, Validation, Visualization, Writing–review and editing. AM: Conceptualization, Data curation, Formal Analysis, Investigation, Methodology, Project administration, Resources, Supervision, Validation, Visualization, Writing–original draft, Writing–review and editing. AT: Conceptualization, Project administration, Resources, Supervision, Writing–review and editing. MT: Conceptualization, Methodology, Project administration, Resources, Supervision, Writing–original draft, Writing–review and editing.

Conflict of interest

Author CK was employed by the company BASF Corporation.

The remaining authors declare that the research was conducted in the absence of any commercial or financial relationships that could be construed as a potential conflict of interest.

The author(s) declared that they were an editorial board member of Frontiers, at the time of submission. This had no impact on the peer review process and the final decision.

Generative AI statement

The author(s) declare that no Generative AI was used in the creation of this manuscript.

Publisher's note

Supplementary material

The Supplementary Material for this article can be found online at: https://www.frontiersin.org/articles/10.3389/fceng.2025.1532384/full#supplementary-material

References

Armellini, F. J., and Tester, J. W. (1993). Solubility of sodium chloride and sulfate in sub- and supercritical water vapor from 450–550°C and 100–250 bar. *Fluid Phase Equilibria* 84, 123–142. doi:10.1016/0378-3812(93)85120-b

Beims, R. F., Hu, Y., Shui, H., and Xu, C. (2020). Hydrothermal liquefaction of biomass to fuels and value-added chemicals: products applications and challenges to develop large-scale operations. *Biomass Bioenergy* 135, 105510. doi:10.1016/j.biombioe.2020.105510

Briones, J. A., Beaton, T. A., Mullins, J. C., and Thies, M. C. (1989). Liquid-liquid equilibria for oleic acid-water mixtures at elevated temperatures and pressures. *Fluid Phase Equilibria* 53, 475–482. doi:10.1016/0378-3812(89)80113-x

Cronin, D., Schmidt, A. J., Billing, J., Hart, T. R., Fox, S. P., Fonoll, X., et al. (2022). Comparative study on the continuous flow hydrothermal liquefaction of various wet-waste feedstock types. *ACS Sustain. Chem. and Eng.* 10, 1256–1266. doi:10.1021/acssuschemeng.1c07214

Doležal, M., and Králová, K. (2011). "Synthesis and evaluation of pyrazine derivatives with herbicidal activity," in *Herbicides, theory and applications*, eds. M. L. Larramendy and S. Soloneski (London, United Kingdom: IntechOpen), 581–610. doi:10.5772/13482

Ellersdorfer, M. (2020). Hydrothermal co-liquefaction of chlorella vulgaris with food processing residues, green waste and sewage sludge. *Biomass Bioenergy* 142, 105796. doi:10.1016/j.biombioe.2020.105796

EPA (2022). *National overview: facts and figures on materials, wastes and recycling*. Available online at: https://www.epa.gov/facts-and-figures-about-materials-waste-and-recycling/national-overview-facts-and-figures-materials (Accessed November 21, 2024).

EPA (2024). *Registration review of pyridine and pyrimidine herbicides*. Available online at: https://www.epa.gov/ingredients-used-pesticide-products/registration-review-pyridine-and-pyrimidine-herbicides (Accessed February 11, 2025).

Hamawand, I. (2023). Energy consumption in water/wastewater treatment industry—optimisation potentials. *Energies* 16, 2433. doi:10.3390/en16052433

He, Z., Xu, D., Wang, S., Zhang, H., and Jing, Z. (2018). Catalytic upgrading of water-soluble biocrude from hydrothermal liquefaction of chlorella. *Energy and Fuels* 32, 1893–1899. doi:10.1021/acs.energyfuels.7b03823

Jamil, A. K., Muraza, O., Osuga, R., Shafei, E. N., Choi, K.-H., Yamani, Z. H., et al. (2016). Hydrothermal stability of one-dimensional pore ZSM-22 zeolite in hot water. *J. Phys. Chem. C* 120, 22918–22926. doi:10.1021/acs.jpcc.6b04980

Karge, H. G. (1991). "Chapter 14 coke formation on zeolites," in *Studies in surface science and Catalysis*. Editors H. van Bekkum, E. M. Flanigen, and J. C. Jansen (Elsevier), 531–570.

Law, Y., Jacobsen, G. E., Smith, A. M., Yuan, Z., and Lant, P. (2013). Fossil organic carbon in wastewater and its fate in treatment plants. *Water Res.* 47, 5270–5281. doi:10.1016/j.watres.2013.06.002

LeClerc, H. O., Tompsett, G. A., Paulsen, A. D., McKenna, A. M., Niles, S. F., Reddy, C. M., et al. (2022). Hydroxyapatite catalyzed hydrothermal liquefaction transforms food waste from an environmental liability to renewable fuel. *iScience* 25, 104916. doi:10.1016/j.isci.2022.104916

Li, B., Liu, C., Bai, J., Huang, Y., Su, R., Wei, Y., et al. (2024). Strategy to mitigate substrate inhibition in wastewater treatment systems. *Nat. Commun.* 15, 7920. doi:10.1038/s41467-024-52364-9

Lok, C. M., Van Doorn, J., and Aranda Almansa, G. (2019). Promoted ZSM-5 catalysts for the production of bio-aromatics, a review. *Renew. Sustain. Energy Rev.* 113, 109248. doi:10.1016/j.rser.2019.109248

Maag, A. R., Tompsett, G. A., Tam, J., Ang, C. A., Azimi, G., Carl, A. D., et al. (2019b). ZSM-5 decrystallization and dealumination in hot liquid water. *Phys. Chem. Chem. Phys.* 21, 17880–17892. doi:10.1039/c9cp01490j

Maag, A. R., Yelvington, P. E., Tompsett, G. A., and Timko, M. T. (2019a). Comparative study of gaseous and high-pressure liquid reactions in industrial chemistry. *Chem. Eng. Process. - Process Intensif.* 145, 107661. doi:10.1016/j.cep.2019.107661

McCusker, L. B., and Baerlocher, C. (2005). "Zeolite structures," in *Studies in surface science and Catalysis*. Editors J. Čejka and H. van Bekkum (Elsevier), 41–64.

Page, J. R., LeClerc, H. O., Smolitsky, P., Esposito, J. P., Theberge, D. P., Zaker, A., et al. (2022). Improving yields and catalyst reuse for palmitic acid aromatization in the presence of pressurized water. *ACS Sustain. Chem. and Eng.* 10, 5659–5673. doi:10.1021/acssuschemeng.2c00665

Rao, U., Posmanik, R., Hatch, L. E., Tester, J. W., Walker, S. L., Barsanti, K. C., et al. (2018). Coupling hydrothermal liquefaction and membrane distillation to treat anaerobic digestate from food and dairy farm waste. *Bioresour. Technol.* 267, 408–415. doi:10.1016/j.biortech.2018.07.064

Ravenelle, R. M., Schüßler, F., D'Amico, A., Danilina, N., van Bokhoven, J. A., Lercher, J. A., et al. (2010). Stability of zeolites in hot liquid water. *J. Phys. Chem. C* 114, 19582–19595. doi:10.1021/jp104639e

Romano, P., Stampone, N., and Di Giacomo, G. (2023). Evolution and prospects of hydrothermal carbonization. *Energies* 16, 3125. doi:10.3390/en16073125

Saleem, M., Tomei, G., Ulucan-Altuntas, K., Grossule, V., Lavagnolo, M. C., Mustafa, A., et al. (2025). Enhanced removal of organics and ammonia from municipal wastewater using an activated carbon/zeolite coupled atmospheric plasma system. *J. Environ. Chem. Eng.* 13, 115459. doi:10.1016/j.jece.2025.115459

Santos, G. O. S., Dória, A. R., Vasconcelos, V. M., Sáez, C., Rodrigo, M. A., Eguiluz, K. I. B., et al. (2020). Enhancement of wastewater treatment using novel laser-made Ti/SnO2–Sb anodes with improved electrocatalytic properties. *Chemosphere* 259, 127475. doi:10.1016/j.chemosphere.2020.127475

Sharma, P., and Melkania, U. (2018). Effect of phenolic compounds on hydrogen production from municipal solid waste. *Waste Manag.* 78, 115–123. doi:10.1016/j.wasman.2018.05.039

Snowden-Swan, L. J., Li, S., Jiang, Y., Thorson, M. R., Schmidt, A. J., Seiple, T. E., et al. (2022). *Wet waste hydrothermal liquefaction and biocrude upgrading to hydrocarbon fuels: 2021 state of technology*. Richland, WA (United States): Pacific Northwest National Lab.PNNL.

Swetha, A., ShriVigneshwar, S., Gopinath, K. P., Sivaramakrishnan, R., Shanmuganathan, R., and Arun, J. (2021). Review on hydrothermal liquefaction aqueous phase as a valuable resource for biofuels, bio-hydrogen and valuable bio-chemicals recovery. *Chemosphere* 283, 131248. doi:10.1016/j.chemosphere.2021.131248

Tait, P. W., Brew, J., Che, A., Costanzo, A., Danyluk, A., Davis, M., et al. (2020). The health impacts of waste incineration: a systematic review. *Aust. N. Z. J. Public Health* 44, 40–48. doi:10.1111/1753-6405.12939

Tam, N. T., and Cooney, R. P. (1976). Vibrational spectra of molecules on zeolites. Part 3.—Raman spectra of pyrazine on zeolites X. *Phys. Chem. Condens. Phases* 72, 2598–2604. doi:10.1039/f19767202598

U. Nations (2022). *Population*. Available online at: https://www.un.org/en/global-issues/population (Accessed November 21, 2024).

Usman, M., Cheng, S., Boonyubol, S., and Cross, J. S. (2024). From biomass to biocrude: innovations in hydrothermal liquefaction and upgrading. *Energy Convers. Manag.* 302, 118093. doi:10.1016/j.enconman.2024.118093

Valenzuela, A. L., Vasquez-Medrano, R., Ibanez, J. G., Frontana-Uribe, B. A., and Prato-Garcia, D. (2017). Remediation of diquat-contaminated water by electrochemical advanced oxidation processes using boron-doped diamond (BDD) anodes. *Water, Air, and Soil Pollut.* 228, 67. doi:10.1007/s11270-017-3244-5

Wang, Y., Guerra, P., Zaker, A., Maag, A. R., Tompsett, G. A., Smith, L. J., et al. (2020). Strategies for extending zeolite stability in supercritical water using thermally stable coatings. *ACS Catal.* 10, 6623–6634. doi:10.1021/acscatal.0c01722

Watson, J., Wang, T., Si, B., Chen, W.-T., Aierzhati, A., and Zhang, Y. (2020). Valorization of hydrothermal liquefaction aqueous phase: pathways towards commercial viability. *Prog. Energy Combust. Sci.* 77, 100819. doi:10.1016/j.pecs.2019.100819

Welsh, J. (2024). Managing TOC and THM risks in drinking water treatment.

Xin, H., Li, X., Fang, Y., Yi, X., Hu, W., Chu, Y., et al. (2014). Catalytic dehydration of ethanol over post-treated ZSM-5 zeolites. *J. Catal.* 312, 204–215. doi:10.1016/j.jcat.2014.02.003

Yaashikaa, P. R., Kumar, P. S., Nhung, T. C., Hemavathy, R. V., Jawahar, M. J., Neshaanthini, J. P., et al. (2022). A review on landfill system for municipal solid wastes: insight into leachate, gas emissions, environmental and economic analysis. *Chemosphere* 309, 136627. doi:10.1016/j.chemosphere.2022.136627

Yang, J., Zhang, J., Du, X., Gao, T., Cheng, Z., Fu, W., et al. (2024). Ammonia inhibition in anaerobic digestion of organic waste: a review. *Int. J. Environ. Sci. Technol.* 22, 3927–3942. doi:10.1007/s13762-024-06029-1

Zaker, A., Tompsett, G. A., Wang, S., Bond, J. Q., and Timko, M. T. (2022). Supercritical water promoted aromatics production using ZSM-5 catalyst. *Fuel* 310, 122360. doi:10.1016/j.fuel.2021.122360

Zhang, L., Chen, K., Chen, B., White, J. L., and Resasco, D. E. (2015). Factors that determine zeolite stability in hot liquid water. *J. Am. Chem. Soc.* 137, 11810–11819. doi:10.1021/jacs.5b07398

Zhu, D., Wang, Z., Liu, K., Si, B., Yang, G., Tian, C., et al. (2023). Multi-cycle anaerobic digestion of hydrothermal liquefaction aqueous phase: role of carbon and iron based conductive materials in inhibitory compounds degradation, microbial structure shaping, and interspecies electron transfer regulation. *Chem. Eng. J.* 454, 140019. doi:10.1016/j.cej.2022.140019